Supplementary Information

84.0% Energy-efficient nitrate conversion by defective $(Fe,Cu,Ni)_2O_3$ electrocatalyst

Tadele Negash Gemeda[1 3], Dong-Hau Kuo[1,2*], Quoc-Nam Ha[1], Noto Susanto Gultom[1], Girma Sisay Wolde[1]

[1] Department of Materials Science and Engineering, National Taiwan University of Science and Technology, No. 43, Sec. 4, Keelung Road, Taipei 10607, Taiwan.

[2] Graduate Institute of Energy and Sustainability Technology, National Taiwan University of Science and Technology, No. 43, Sec. 4, Keelung Road, Taipei 10607, Taiwan.

[3] Department of Chemical Engineering, Adama Science and Technology University, P.O. Box 1888 Adama, Ethiopia.

*Corresponding author

Fax: +011-886-2-27303291. E-mail: dhkuo@mail.ntust.edu.tw

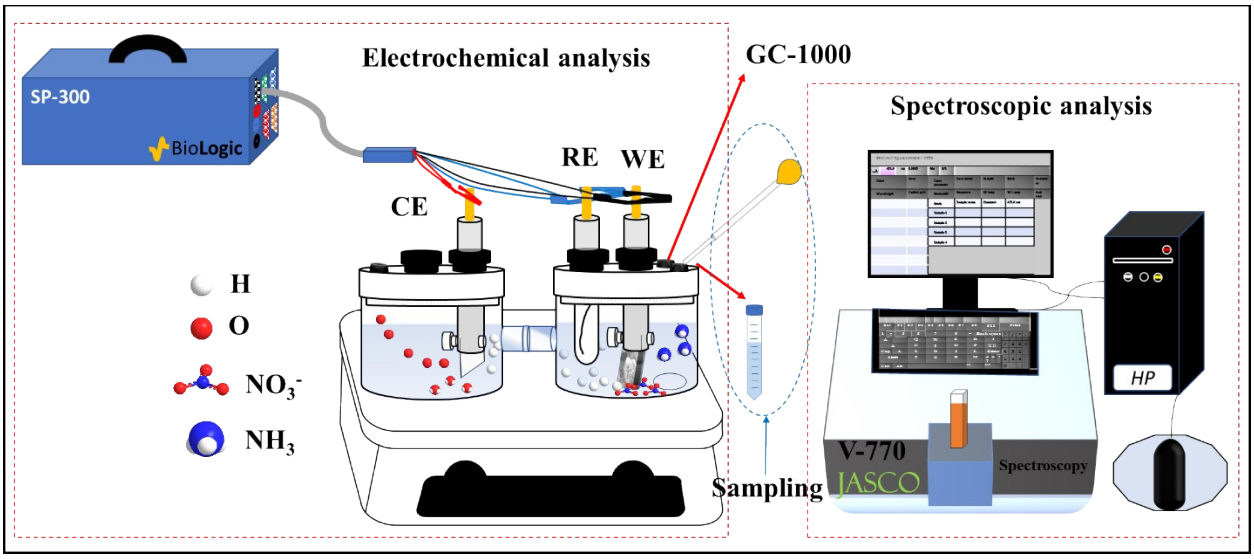

Figure S1. Batchwise H-cell compartment configuration for electrochemical analysis with the corresponding spectroscopic measuring setup.

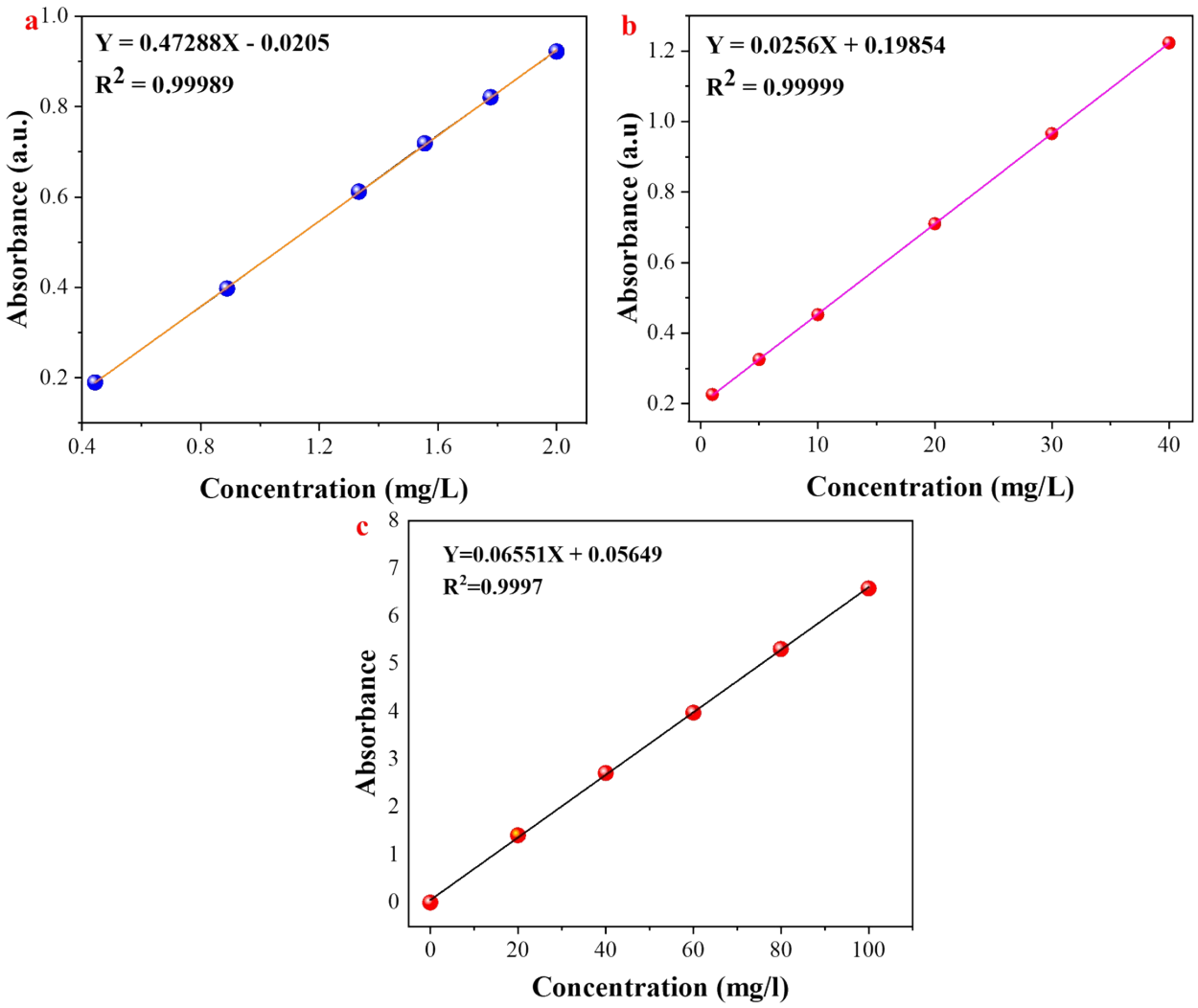

Figure S2. UV-Vis calibration for (a) NH_3, (b) NO_2^-, and (c) N_2H_4 detection.

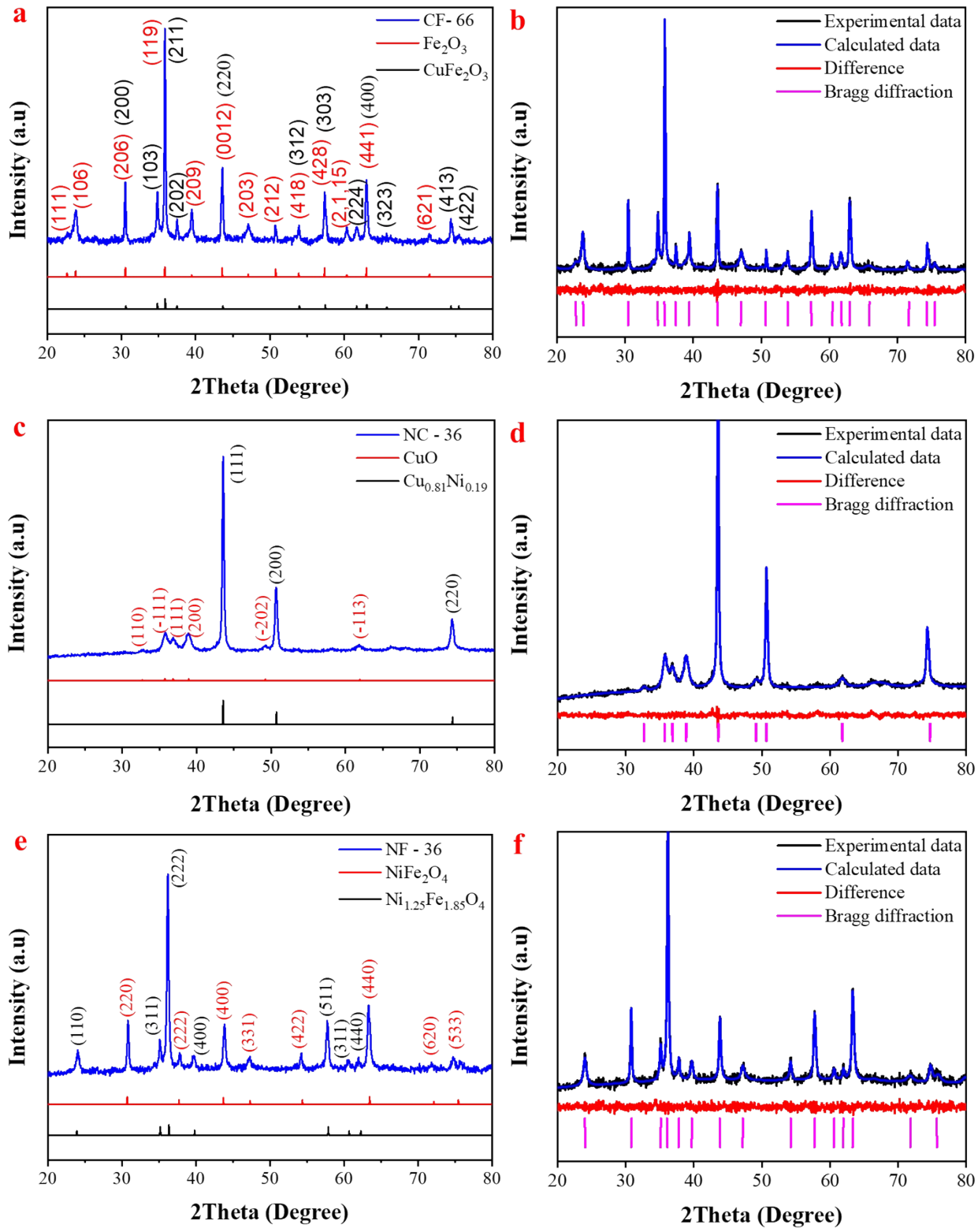

Figure S3. X-ray diffraction (XRD) pattern and the corresponding Rietveld refinement for bimetallic-oxide system (a-b) CF-66, (c-d) NC-36, and (e-f) NF-36.

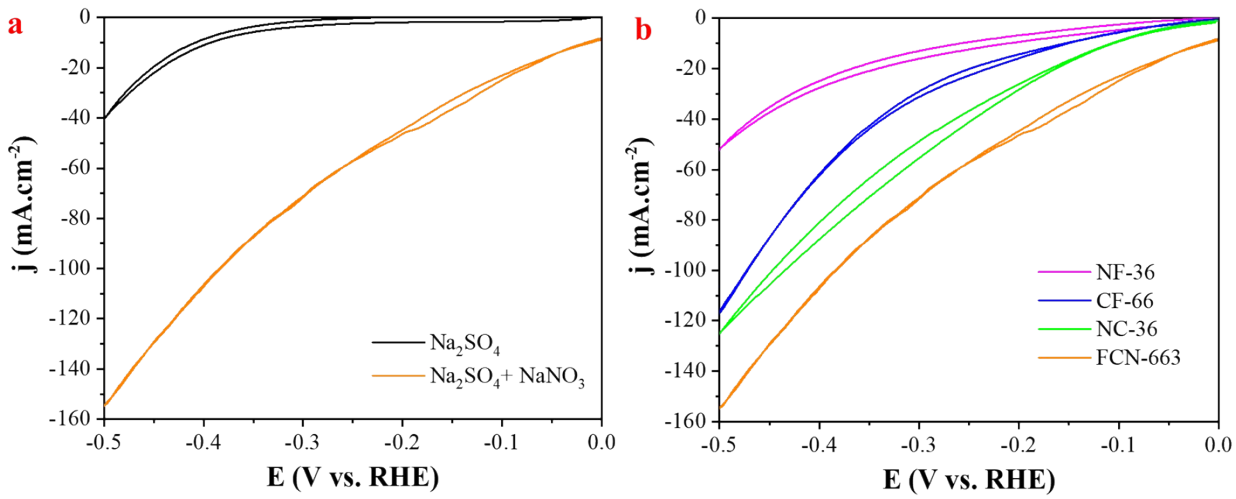

Figure S4. (a) CV curves of FCN-663 metal-oxide system in Na_2SO_4 electrolyte with and without $NaNO_3$, (b) CV curves of ternary metallic oxide system (FCN-663) with the bimetallic system (NC-36, CF-66, and NF-36).

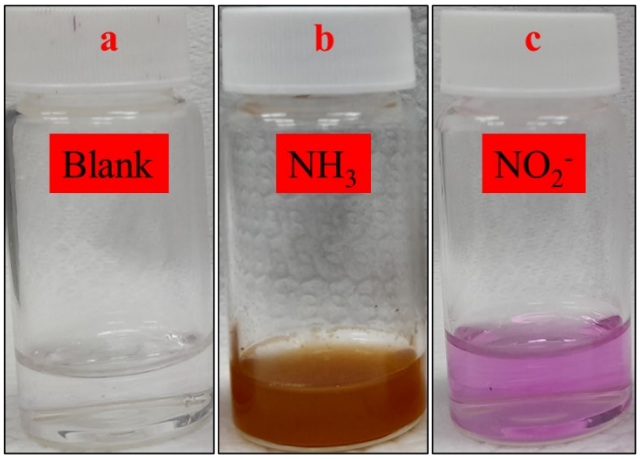

Figure S5. The appearance of nitrate reduction product and by-product, (a) Blank, (b) NH_3, and (c) NO_2^-, of a ternary FCN-663 metal-oxide system after a 2 h batch reaction at -0.3 V vs. RHE using H-cell.

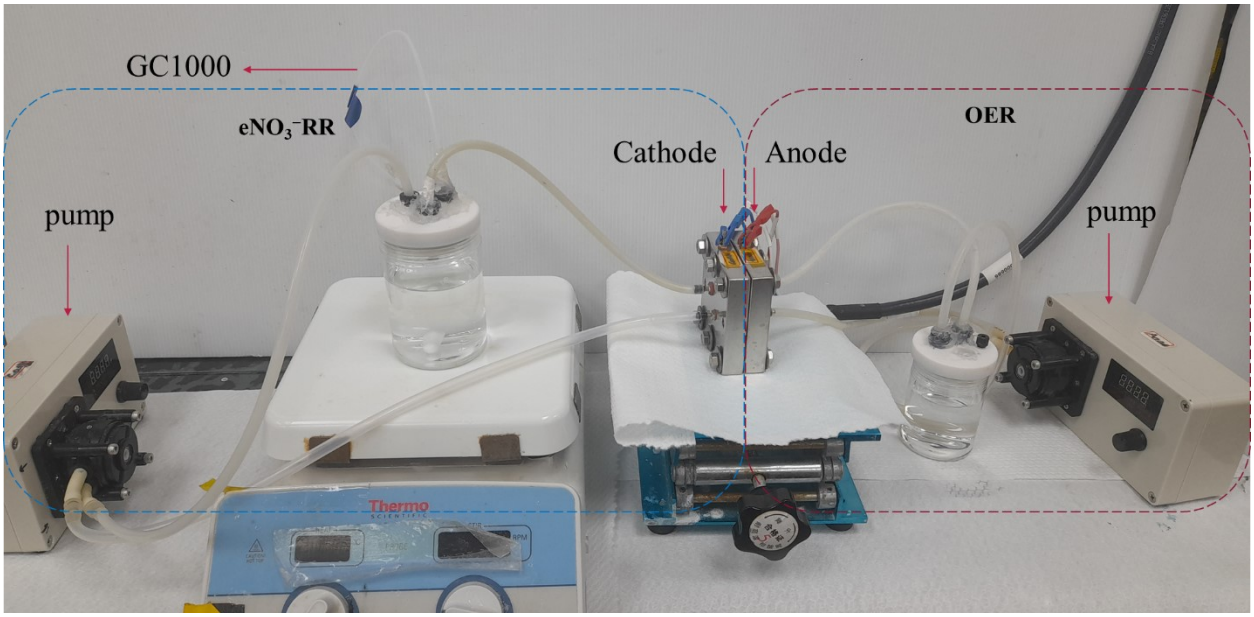

Figure S6 Single-stack flow cell electrolyzer set-up.

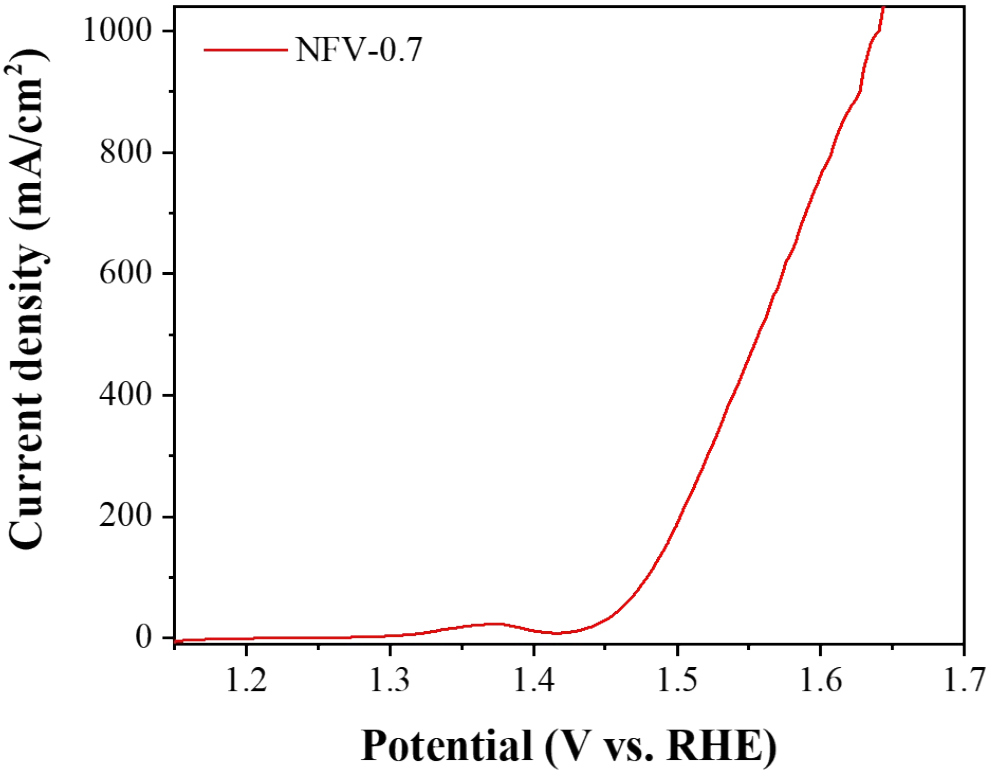

Figure S7. LSV curve of NFV-0.7 (previously prepared by our group) as OER electrode for anode side.

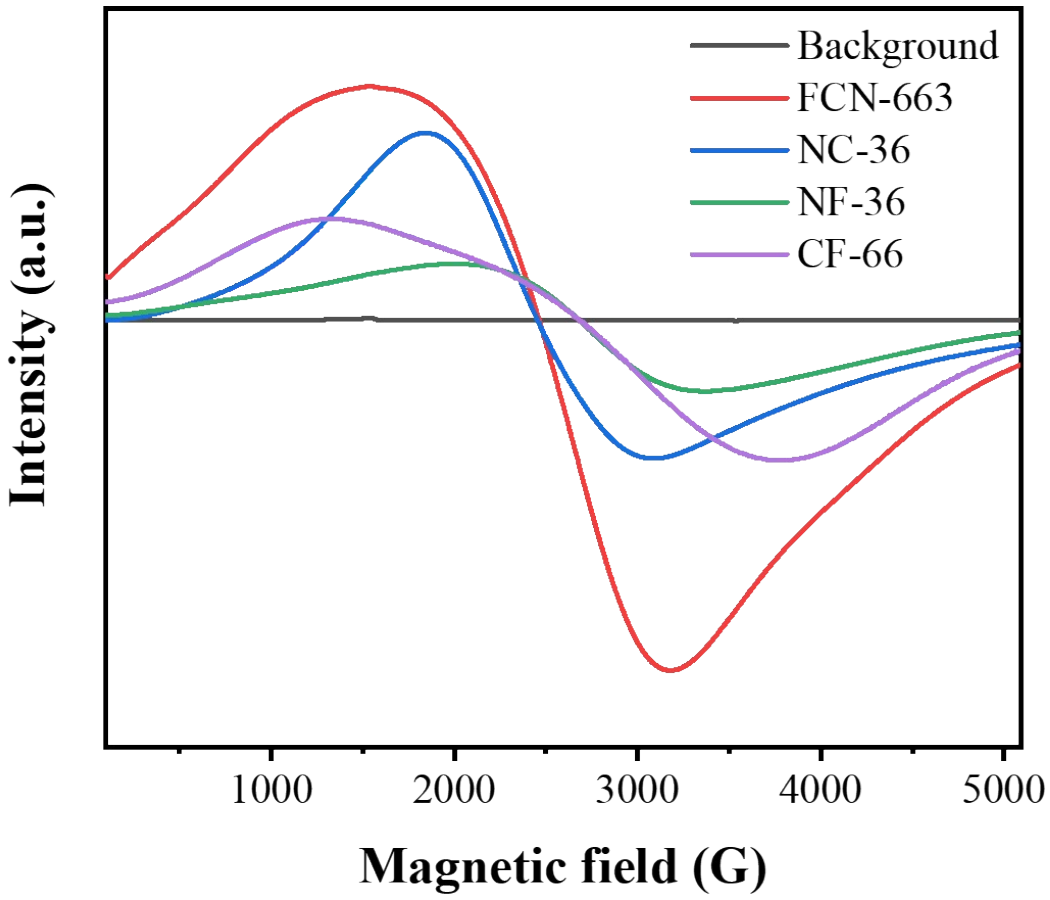

Figure S8. EPR spectra of the trimetallic oxide system (FCN−663) and the bimetallic systems (NC-36, CF-66, and NF-36).

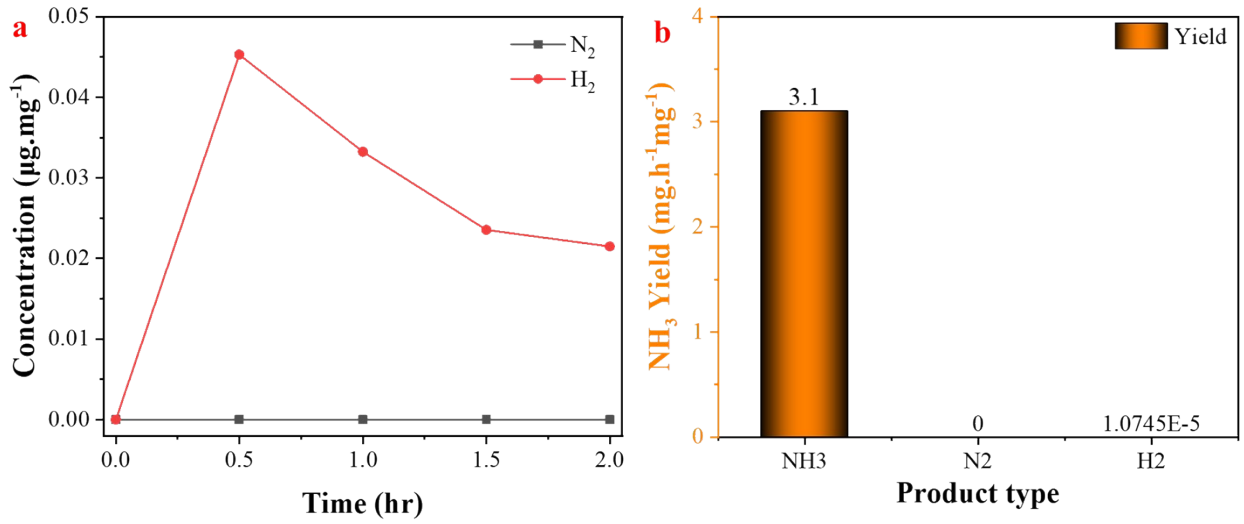

Figure S9. By product analysis and comparison, a) concentration vs. reaction time and b) yield vs. product type (NH_3, N_2, and H_2) of a ternary FCN−663 metal-oxide system after a 2 h reaction at -0.3 V vs. RHE.

Table S1. Synthesized materials system naming and their sample size with mass loading

No.	Catalyst	Ratio (in mmol)	Labeling	Weight (mg)	Sample size (cm^2)
1	Fe-Cu-Ni	6:6:3	FCN-663	3	1x1
2	Ni-Cu	3:6	NC-36	2.53	1x1
3	Cu-Fe	6:6	CF-66	2.82	1x1
4	Ni-Fe	3:6	NF-36	2.61	1x1

Table S2. Lattice parameter, cell volume, and angle of bimetallic and trimetallic metallic oxide systems

Samples	XRD phase	Lattice parameter		Cell volume	Angle, β
		A (Å)	**c (Å)**	V ($Å^3$)	
CF-66	Fe_2O_3	4.913	14.128	295.43	57.86
	$CuFe_2O_4$	5.93	8.65	304.78	1.91
NC-36	$CuO_{0.81}NiO_{0.19}$	3.619	-	47.4	17.7
	CuO	4.8846	4.1357	96.5661	21.5
NF-36	$Ni_{1.25}Fe_{1.85}O_4$	8.52902	-	620.43	25.4
	$NiFe_2O_4$	8.3189	-	575.72	81.03
FCN-663	Fe_2O_3	5.17959	13.73	304.289	508.74
	$Cu_{0.81}Ni_{0.19}$	4.03018	-	65.459	19.1

Table S3. XPS compositional analysis of the FCN-663 oxide system grown on Ni foam

Element	Ni	Cu	Fe	O
at. %	12.69	17.67	15.93	53.72

Table S4. Valence state proportion of FCN-663 through the deconvoluted peak fitting of XPS peak area

Element	**Ni**		**Cu**	**Fe**		**O**		
	Ni^{2+}	Ni^{3+}	Cu^{+}	Fe^{2+}	Fe^{3+}	O_L	O_V	O_{ads}
at.%	17.72	82.28		33.74	66.26	59.63	37.15	3.23
Data from Table S3 (%)	2.25	10.44	17.67	5.38	10.56	32.03	19.96	1.74

Table S5. Comparison of NH_3 yield and Faradic efficiency (FE) of the reported electrocatalysts with good performance

Catalyst	Electrolyte	Potential V vs. RHE	Catalyst amount	NH_3 Yield	FE (%)	Ref.
Fe_2O_3/ $Cu_{0.81}Ni_{0.19}$ nanoflower	0.5 M Na_2SO_4 (168 ppm $NaNO_3$)	− 0.3	3 mg 1 cm^2	9.18 $mg.h^{-1}.cm^{-2}$ 3.06 $mg.h^{-1}.mg_{cat}^{-1}$ 0.54 $mmol\ h^{-1}.cm^{-2}$	94.79	This work
Cu–Fe_2O_3-*x*	0.5 M Na_2SO_4 (50 ppm NO_3^-)	− 0.6	0.89 mg cm^{-2}	0.108 $mmol\ h^{-1}.cm^{-2}$ 1.836 $mg\ h^{-1}.cm^{-2}$	80.1	[1]
Cu/Cu_2O NWAs	0.5 M Na_2SO_4 (200 ppm Na_2SO_4)	− 0.85	1 cm^2	0.2449 $mmol\ h^{-1}.cm^{-2}$ 4.1633 $mg\ h^{-1}.cm^{-2}$	95.8	[2]
Cu-Ni alloys	0.1 M Na_2SO_4 (0.01 M $NaNO_3$)	− 0.7	0.25 cm^2	--	94.56	[3]
CuNi/NC-51	0.05 M Na_2SO_4 (50 ppm NO_3^-)	− 1	2.25 cm^2	-	79.6	[4]
CoP/TiO_2	0.1 M NaOH ($NaNO_3$)	− 0.3	0.25 cm^2	297.2 $\mu mol\ h^{-1}.cm^{-2}$ 5.0524 $mg\ h^{-1}.cm^{-2}$	95	[5]
$Cu_{49}Fe_1$	0.1 M K_2SO_4 (2 mM KNO_3)	− 0.74	0.196 cm^2	0.23 $mmol\ h^{-1}.cm^{-2}$ 3.91 $mg\ h^{-1}.cm^{-2}$	94.5	[6]
Ni/Cu_2O/ $Co(OH)_x$	12.5 mM Na_2SO_4 (30 mg/L NO_3^-)	40 $mA.cm^{-2}$	2.25 cm^2	1.22 $mmol\ g_{cat}^{-1}$ 20.74 $mg\ h^{-1}.g_{cat}^{-1}$ 0.0207 $mg\ h^{-1}.mg_{cat}^{-1}$	22	[7]
Cu–Fe_3O_4	0.05 M Na_2SO_4 (100 mg/L NO_3^-)	25 mA/cm^2	4 cm^2	-	50.3	[8]
$NiFe_2O_4$/ CC	0.1 M PBS (0.1 M $NaNO_3$)	− 0.6	-	2.98 $mg.h^{-1}.cm^{-2}$ @-0.6 10.6 $mg.h^{-1}.cm^{-2}$ @ −1.0 V	96.6	[9]
Fe-Co_3O_4 NA/TM	0.1 M PBS (50 mM NO_3)	− 0.7	1 cm^2	0.624 $mg\ h^{-1}.mg_{cat}^{-1}$	95.5	[10]
Au_1Cu (111)	0.1 M KOH (7.1 mM KNO_3)	− 0.2	3 cm^2	0.55 $mg\ h^{-1}.cm^{-2}$	97	[11]
10 Cu/ TiO_{2-x}	0.5 M Na_2SO_4 (3.2 mM $NaNO_3$)	− 0.75	3 cm^2	1.94 $mg\ h^{-1}.cm^{-2}$ 0.1143 $mmol\ h^{-1}.mg^{-1}$	81.34	[12]

Reference

1. Y. Gao, K. Huang, C. Yan, S. Li, H. Zhang, L. Cheng and F. Huang, *Mater. Adv.*, 2022, **3**, 7107-7115.
2. Y. Wang, W. Zhou, R. Jia, Y. Yu and B. Zhang, *Angew. Chem. Int. Ed.*, 2020, **59**, 5350-5354.
3. Z. Bai, X. Li, L. Ding, Y. Qu and X. Chang, *Science China Materials*, 2023, **66**, 2329-2338.
4. Y. Liu, B. Deng, K. Li, H. Wang, Y. Sun and F. Dong, *J Colloid Interf Sci*, 2022, **614**, 405-414.
5. Z. Deng, C. Ma, X. Fan, Z. Li, Y. Luo, S. Sun, D. Zheng, Q. Liu, J. Du, Q. Lu, B. Zheng and X. Sun, *Materials Today Physics*, 2022, **28**, 100854.
6. C. Wang, Z. Liu, T. Hu, J. Li, L. Dong, F. Du, C. Li and C. Guo, *ChemSusChem*, 2021, **14**, 1825-1829.
7. G. A. Cerrón-Calle, A. Wines and S. Garcia-Segura, *Appl. Catal. B*, 2023, **328**, 122540.
8. Z. Zhang, G. Xin, Y. Pan, Z. Chen, Y. Sun, C. Wang, S. Li, L. Wei, Z. Fu and W. Ma, *Journal of Cleaner Production*, 2023, **383**, 135388.
9. L. Xie, L. Hu, Q. Liu, S. Sun, L. Zhang, D. Zhao, Q. Liu, J. Chen, J. Li, L. Ouyang, A. A. Alshehri, Q. Kong and X. Sun, *Inorganic Chemistry Frontiers*, 2022, **9**, 3392-3397.
10. P. Wei, J. Liang, Q. Liu, L. Xie, X. Tong, Y. Ren, T. Li, Y. Luo, N. Li, B. Tang, A. M. Asiri, M. S. Hamdy, Q. Kong, Z. Wang and X. Sun, *J Colloid Interf Sci*, 2022, **615**, 636-642.
11. Y. Zhang, X. Chen, W. Wang, L. Yin and J. C. Crittenden, *Applied Catalysis B: Environmental*, 2022, **310**, 121346.

12. X. Zhang, C. Wang, Y. Guo, B. Zhang, Y. Wang and Y. Yu, *J Mater Chem A*, 2022, **10**, 6448-6453.